21st International Congress on Modelling and Simulation, Gold Coast, Australia, 29 Nov to 4 Dec 2015
www.mssanz.org.au/modsim2015

Pyroconvective interaction of two merged fire lines: curvature effects and dynamic fire spread

C.M. Thomas [a], **J.J. Sharples** [a b] **and J.P. Evans** [c]

[a]*Applied and Industrial Mathematics Research Group, School of Physical, Environmental and Mathematical Sciences, UNSW Canberra, Australia*
[b]*Bushfire and Natural Hazards Cooperative Research Centre, Australia*
[c]*Climate Change Research Centre, University of New South Wales, Australia*

Email: christopherthomas@cmt.id.au

Abstract: The interaction of one fire with another can substantially alter the behaviour of the individual fires. This may occur, for example, during the coalescence of spot fires or when separate fire fronts merge. The resulting fire-fire interactions may lead to unexpected, and in some cases extreme, fire behaviour. One manifestation of this behaviour is a change in the rates of spread of the individual fires. Viegas et al. (2012) studied this effect analytically and experimentally in the case of the intersection of two line fires meeting at an acute angle, and have reported on the so-called 'jump fire' phenomenon whereby initially the fire front in the vicinity of the intersection of the two fires advances very rapidly. They interpreted this as a rotation of the lines of fire, however it may also be interpreted in terms of the curvature of the merged fire front. Indeed, Sharples et al. (2013) were able to qualitatively reproduce the 'jump fire' behaviour using a simple numerical model of frontal evolution in which the rate of spread in the normal direction is dependent on the curvature of the fire line. Such curvature dependent flows occur elsewhere in nature, for example in the growth of crystals and in gas-phase flame propagation, and have been studied extensively (Sethian, 1985). In the context of wildfire, possible mechanisms for such an effect include atmosphere-fire interactions and geometric effects relating to the radiative and convective transfer of energy. The inclusion of curvature dependence may be a tractable way to incorporate the effects of these complex phenomena into models of fire spread that do not currently accommodate them. To determine the extent to which this curvature effect is captured by a coupled atmosphere-fire model (WRF-Fire) we perform numerical experiments and analyse the relationship between the rate of spread and the curvature of the modelled front. This study focuses on geometric configurations of fires similar to those considered by Viegas et al. (2012).

The coupled atmosphere-fire simulations produced patterns of fire propagation that were qualitatively similar to those reported by Viegas et al. (2012). This is despite a significant difference in the spatial scales of the two studies: the experiments of Viegas et al. (2012) considered fire lines a few metres in length, while those considered here are about one kilometre long. The main feature of the coupled simulations was the formation of a strong convective updraft between the two fire lines near their point of intersection, which caused that part of the merged fire to advance more rapidly. Comparisons with simulations in which the two fire lines were allowed to burn independently indicated that pyroconvective coupling between the two fire lines increased the overall rate of advance of the intersection point by a factor of about 7-10. As such, the simulations suggest that a fire spreading under similar scenarios will propagate with a considerable dynamic element.

Local fire-line curvature was calculated and compared with instantaneous rates of spread to test the hypothesis that the rapid advance of the point of intersection can be thought of as a curvature effect. This comparative analysis did not find that large negative curvature is associated with higher rates of spread; in fact the highest rates of spread in the simulations were consistently associated with parts of the fire line with local curvature very close to zero. However, the analysis presented here does not rule out the existence of such a curvature effect in some mean sense.

Keywords: *Dynamic fire spread, curvature, coupled fire-atmosphere modelling, fire line merging*

1 INTRODUCTION

1.1 Dynamic fire behaviour

In recent years, southeastern Australia has been impacted by a number of bushfires which have exhibited fire behaviour that has been difficult to reconcile with current fire modelling paradigms. Changing weather conditions and variations in terrain and fuel can produce erratic fire behaviour that is difficult to predict. Even in uniform conditions of fuel, weather and terrain, interactions between the fire and the environment, as well as between separate fires, can produce dynamic modes of fire propagation resulting in irregular and unpredictable fire behaviour. This has obvious implications for people on the ground and is therefore of great interest to operational personnel as well as wildfire researchers. Examples of dynamic modes of fire spread include those considered by Viegas (2005), Sharples et al. (2012) and Simpson et al. (2013), while other examples involving intrinsic fire dynamics include the types of behaviour exhibited when spot fires coalesce or when obliquely intersecting fire lines merge with one another (Viegas et al., 2012). Dynamic modes of fire propagation remain poorly understood, and are not accounted for in the current suite of operational fire spread models.

1.2 Fire-spread models

Much of the difficulty of modelling wildfire behaviour arises from the range of scales that the phenomena span, from the millimetre-scale combustion of individual fuel elements to pyrogenic atmospheric phenomena at scales of the order of a kilometre, and large fires with tens of kilometres of fire line. Physical models attempt to explicitly represent the physical and chemical processes involved but computational constraints make it impossible to do this at all scales, and they are not able to model even moderately sized wildfires. Empirical models, like those of McArthur (1966; 1967), as formulated by Noble et al. (1980), and semi-empirical models like that of Rothermel (1972) are essentially scale-free; the fuel bed is treated as amorphous and locally homogeneous, although phenomena at the scale of a fuel element may play a role in the derivation of a semi-empirical model. Consequently, empirical models (henceforth we use the term ‘empirical’ to encompass both empirical and semi-empirical models) are not subject to the same computational constraints as physical models. However, when used in isolation they can at best predict the mean behaviour of a fire under steady-state conditions. While they may perform well in some circumstances, they do not incorporate the influence of the fire on the atmosphere, they do not explicitly include short-range radiative and convective heat transfer, and they ignore the geometry of the fire line (in the Rothermel model it is assumed to be straight and infinitely long). Thus they are not able to represent dynamic fire behaviour which arises through atmosphere-fire interactions and intrinsic fire dynamics.

Coupled atmosphere-fire models, on the other hand, do represent atmosphere-fire interactions. They are an important tool in wildland fire research, both as an aid in understanding the fundamental processes involved, and because they hold the promise of better operational tools as the models mature and computing technology improves. Some models, such as FIRETEC (Linn et al., 2002), couple a physical fire model with an atmospheric model. These are important research tools for studying detailed fire processes, but they are limited to relatively small domains by their substantial computational cost. Others involve the coupling of an empirical fire-spread model with a physical atmospheric model. Examples of these include CAWFE (Coen, 2013), Méso-NH / ForeFire (Filippi et al., 2009), and WRF-Fire (Coen et al., 2013). In such frameworks the atmosphere may be explicitly modelled at scales down to the order of tens of metres but the fire itself is represented by an empirical model. While this is a compromise over a full physical model, it gives a significant advantage in terms of computational expense. Furthermore the coupling between the atmosphere and fire components means that the models are able to represent dynamic fire behaviour, which is generated, at least in part, by the interaction between the atmosphere and the fire.

1.3 Motivation for the current work

Although coupled models enjoy an advantage over full physical models in terms of computational cost, they are still expensive to run and thus unsuited to field use. Empirical models therefore still have an important role despite not being able to represent dynamic fire behaviour. One might ask if there are ways to include some aspects of dynamic fire behaviour in empirical models even though they are unable to represent the physical processes that cause such behaviour. In addition, coupling with an atmospheric model does not overcome all of the limitations of empirical models discussed earlier. The question then arises as to the extent that coupled models can describe the dynamic fire behaviour that is observed in both experiments and in actual wildfires.

A series of experiments by Viegas et al. (2012) treated the case of the merging of two oblique lines of fire.

The authors reported on the so-called 'jump fire' behaviour where the merged front initially spreads rapidly, before slowing. Viegas et al. provided an analytical treatment of this phenomenon in terms of the 'rotation' of the firelines (see Viegas et al. (2012) for an explanation of this notion) and the accumulation of energy between them. Sharples et al. (2013) gave an alternative heuristic treatment using a very simple model with a rate of spread depending only on fire-line curvature, and were able to reproduce qualitatively the experimental results of Viegas et al. In this context 'curvature' refers to *signed* curvature; negative curvature corresponds to a region concave with respect to the unburnt fuel. A relationship between rate of spread and fire-line curvature has been discussed by a number of authors: Weber (1989), Fendell and Wolff (2001), Sharples et al. (2013), Wheeler et al. (2013). Intuitively, regions of the fire line with negative curvature surround pockets of unburnt fuel. Radiative and convective processes of heat transfer might be expected to lead to a concentration of energy for the drying and ignition of fuel in such regions, with a consequent increase in the rate of spread.

In the current work WRF-Fire is used to model fires with a similar geometric configuration to those of Viegas et al. (2012). The aims are to examine the extent to which the behaviour reported by Viegas et al. is reproduced by the WRF-Fire model, and to determine if there is a relationship between the rate of spread and the curvature of the fire line in the model output.

2 MODELLING SET UP

2.1 WRF-Fire

WRF-Fire (Coen et al., 2013) is implemented as a physics module within the WRF atmospheric model (Skamarock et al., 2008). It couples WRF with the Rothermel fire-spread model (Rothermel, 1972): WRF provides a surface wind field for input to the fire-spread model, and the fire-spread model supplies heat and moisture, in the form of sensible and latent heat fluxes, to WRF. Tracking of the fire front is handled using a level set method (Sethian, 1999). The model output includes the values of the level set function $\varphi(x, y, t)$ which can be used to compute both the position and curvature of the modelled front at any time step: the front at time t is given by $\{(x, y) : \varphi(x, y, t) = 0\}$ and the curvature of any level set is given by (Sethian, 1999)

$$\kappa = \frac{\varphi_{xx}\varphi_y^2 - 2\varphi_x\varphi_y\varphi_{xy} + \varphi_{yy}\varphi_x^2}{(\varphi_x^2 + \varphi_y^2)^{3/2}}, \tag{1}$$

which can be approximated from the model output with finite differences. This is how the local curvature of the fire line is computed in the analysis described in this paper.

For simplicity, in the rest of this paper we will use the term WRF-Fire to denote the complete coupled model which includes WRF and the WRF-Fire physics module.

2.2 Experimental setup

Atmosphere. The WRF-Fire model was run in a domain of 5000 × 5000 × 2000 metres (l × w × h) with a horizontal resolution of 50 × 50 metres and a stretched vertical coordinate with a resolution ranging from around 4 metres at the surface to 170 metres at the model top, with the lowest level at about 2 metres. The model was initialised with no moisture, zero wind speed, and with a neutral layer of constant 300 K potential temperature up to 1000 metres, topped by a stable layer with a constant lapse rate of 6 K per km to the model top. All model physics options were switched off, and the WRF 1.5 order TKE turbulence closure scheme was employed. A constant zero sensible heat flux was assumed at the surface (apart from that generated by the fire model), and a constant drag coefficient of 0.005 was used, corresponding to a surface roughness of 0.03 metres (Coen et al., 2013). Open boundary conditions were used on the lateral boundaries. The surface was taken to be flat and the surface winds, for input into the fire model, were computed at 1 metre above ground level (agl) The flat surface and zero ambient wind is consistent with the experiments of Viegas et al. (2012), which were conducted indoors. At this resolution the WRF model is capable of resolving large turbulent eddies. However there was no intention to conduct these numerical experiments in a developed turbulent convective boundary layer, and this is the reason for setting the surface heat flux to zero. The concern here is not with trying to model 'V'-shaped fires in a realistic way, but rather with examining the extent to which the atmosphere-fire coupling can produce the dynamic fire interactions reported by Viegas et al. (2012). Near-surface horizontal winds produced by large eddies confuse the issue and make it more difficult to isolate the effects of small-scale fire-atmosphere interactions.

Fire. Four geometric configurations were studied, corresponding to those in the experimental setup of Viegas et al. (2012): two oblique fire lines forming a 'V'-shape with included angles of 10°, 20°, 30° and 45°. The

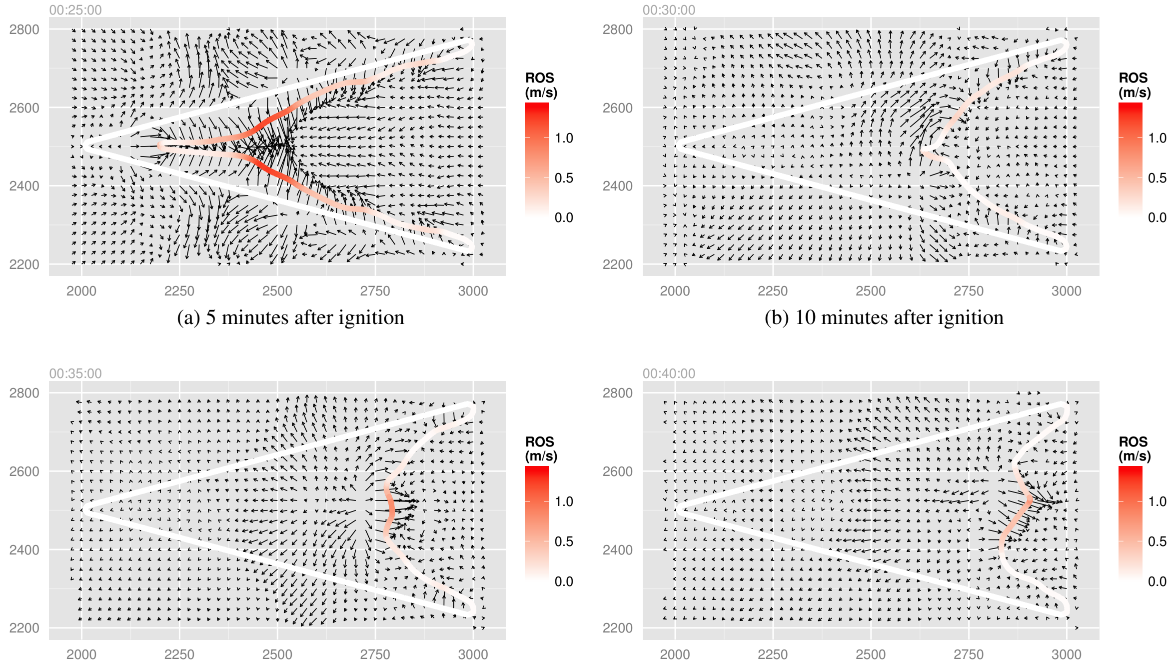

(a) 5 minutes after ignition

(b) 10 minutes after ignition

(c) 15 minutes after ignition

(d) 20 minutes after ignition

Figure 1. Fire line modelled by WRF-Fire for 30° configuration, shown 5, 10, 15 and 20 minutes after ignition. Arrows depict modelled winds at 1 metre agl. Only a portion of the computational domain is shown.

fire lines were each 1000 metres long and positioned so that the centroid of the triangular region formed by the fire lines was located at the centre of the 5×5 kilometre computational grid. Fuel was confined to a triangular region just slightly larger (by 10 metres) in each direction, and the fuel load was set to zero elsewhere. This was done so as to loosely conform with the experimental setup of Viegas et al. (2012) and also to focus attention on the behaviour in the region of interaction between the fire lines. The fuel type used was Category 3 (long grass) of the 13-category Anderson fuel model system (Anderson, 1982). After 20 minutes of model time the fire lines were ignited simultaneously over their entire length and the model was run for a further 30 minutes with data output every 30 seconds. The resolution of the computational fire grid was 5 metres.

3 RESULTS

3.1 Curvature and rate of spread

Figure 1 depicts the modelled fire lines of the 30° configuration at four distinct instants after ignition, along with the modelled winds at 1 metre agl. An association of large negative curvature with higher rates of spread is not evident here. Figure 1 shows only four timesteps of one initial configuration, but in Figure 2 the instantaneous rate of spread of the fire line is plotted against its local curvature for each of the four configurations and all time steps after ignition. The data are extracted from the inner part of the triangular region formed by the initial fire lines because fuel exists only in this region. To remove a few outlying points, which make visualisation difficult, the data have been restricted by including only those with $\kappa \in (-0.01, 0.01)$. Again there is no evidence that higher rates of spread are associated with large negative curvature; indeed, they appear to be associated with curvature close to zero. However this analysis is somewhat crude: at any model output time the rate of spread at a point on the fire line was simply matched with the local curvature of the fire line at the same location. There are at least two possible ways to refine the analysis: one could examine the possibility that there is a lag between the time that the pocket of negative curvature forms and the increase in the rate of spread that eventually fills it, and one could search for a relationship between mean rates of spread and mean fire-line curvature, or perhaps between the rate of spread and curvature of some sort of 'mean' fire line. The sense in which these means should be taken is not clear, but will form the basis of future work.

The deep pocket in the fire line evident in Figure 1(a) may not be physical; there is some suggestion that it might be an artifact relating to the resolution of the computational grids. Future work will include a test of the sensitivity of these results to increased grid resolution, although at 50 metres (atmosphere) and 5 metres (fire)

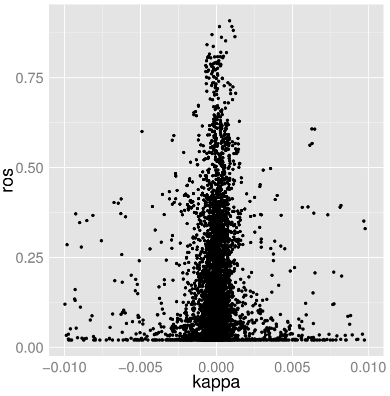

(a) 10°

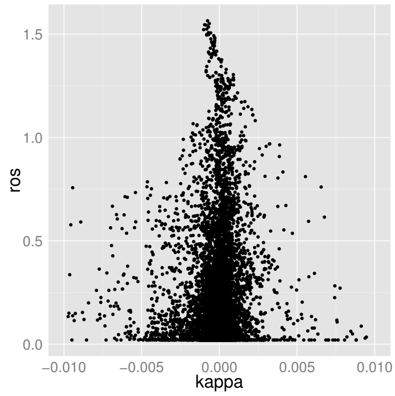

(b) 20°

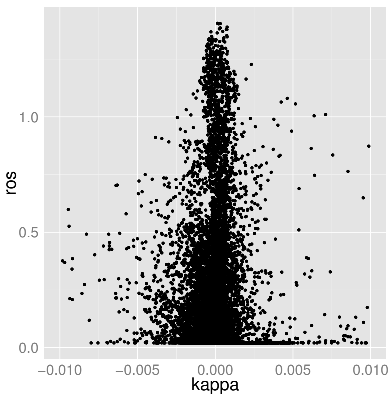

(c) 30°

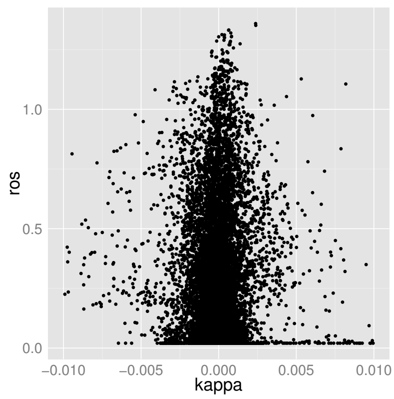

(d) 45°

Figure 2. Rate of spread versus signed curvature κ from the model output for the four configurations studied. The data are points on the fire front interior to the triangular region formed by the oblique lines, and for ease of interpretation the data have been restricted to those with $\kappa \in (-0.01, 0.01)$. All time steps after ignition are represented. There is no association of higher rates of spread with large negative κ apparent in these figures.

these are by no means low resolution runs.

3.2 Representation of dynamic fire behaviour

It is clear from Figure 1 that the model has captured the main features reported in Viegas et al. (2012): a rapid initial acceleration and subsequent slow down of the merged fire line, and a 'rotation' of the original fronts. The results for the other three initial fire-line configurations are quite similar. Viegas et al. attribute this behaviour to 'energy concentration between the fire lines', but its appearance in the WRF-Fire output can only be a result of small-scale atmospheric circulations resulting from the interaction between the fire and the atmosphere. There is a strong updraft just ahead of the fire line which is not shown here (it can be inferred from the convergence of the wind vectors in, for example, Figure 1(a)). This forms soon after ignition and persists for almost 10 minutes, but does not form when the fire lines are ignited individually. It seems likely that the initial rapid acceleration of the front is associated with this feature; it is an example of the dynamic fire behaviour referred to in Section 1.1. Future work will include a study of the vorticity in this region, and an analysis of the mechanism by which this feature forms and persists.

Figure 3 is a composite plot showing the evolution of the fire fronts when the initial fire lines are ignited individually, and when both are ignited simultaneously. This is a dramatic illustration of the effect of the interaction between the fire lines, and of the 'jump fire' behaviour reported by Viegas et al. (2012).

4 DISCUSSION AND CONCLUSION

Dynamic wildfire behaviour is of great interest to both researchers and operational personnel. Empirical models of fire spread, when used in isolation, cannot model such behaviour. However coupled atmosphere-fire

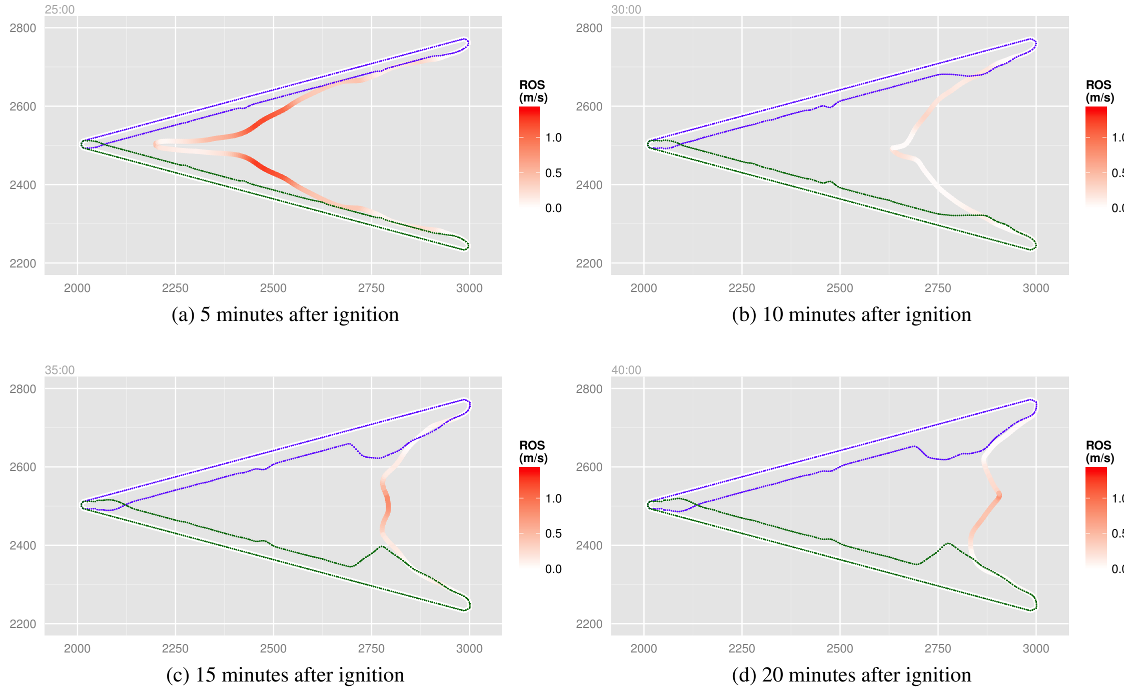

(a) 5 minutes after ignition

(b) 10 minutes after ignition

(c) 15 minutes after ignition

(d) 20 minutes after ignition

Figure 3. Composite plot of fire-line evolution from three model runs made with WRF-Fire under the same conditions as Figure 1. The blue line illustrates the evolution of the front after only the northern arm is ignited, i.e. with no fire-fire interaction. The green line is the corresponding front for the southern arm. The red and white line, identical to that in Figure 1, shows the front when both arms are ignited simultaneously.

models can represent dynamic behaviour even if the fire component of the model assumes the existence of an empirically-defined quasi-steady state.

The dynamic behaviour of a fire in the region between two merging fire lines has been studied experimentally and with a simple analytical model by Viegas et al. (2012). In the current study it has been shown that the behaviour is reproduced well by a coupled atmosphere-fire model, WRF-Fire, despite the limitations of the empirical fire-spread component of the model. However, because of their computational expense, coupled models are not yet suited to use in operational settings. Sharples et al. (2013) showed that the behaviour observed by Viegas et al. (2012) could be represented qualitatively using a simple model of curvature-dependent rate of spread. If a robust relationship between curvature and rate of spread could be established then this might be a way of incorporating dynamic phenomena into operational models that cannot currently accommodate them. An initial analysis of the WRF-Fire model output did not reveal an association of negative local fire-line curvature with higher rates of spread. However there are more sophisticated approaches that have not yet been explored; for example a relationship may exist in some mean sense.

Future work will include a more detailed analysis of the small-scale atmospheric circulations, as represented in WRF-Fire, that lead to this behaviour; a study of the sensitivity of the results to the resolution of the computational grid; and a more sophisticated analysis of any relationship between fire-line curvature and rate of spread.

Acknowledgement

This work was undertaken with the assistance of resources provided by the NCI National Facility at the Australian National University through the National Computational Merit Allocation Scheme supported by the Australian Government. J.J. Sharples (IN130100038, IN140100011) and J.P Evans (FT110100576) acknowledge the support of the Australian Research Council.

References

Anderson, H. E. (1982). Aids to Determining Fuel Models For Estimating Fire Behavior. Technical report, Forest Service, United States Department of Agriculture, Ogden, Utah.

Coen, J. (2013). Modeling Wildland Fires: A Description of the Coupled AtmosphereWildland Fire Environment Model (CAWFE). Technical report, National Center for Atmospheric Research, Boulder, Colorado, USA.

Coen, J. L., M. Cameron, J. Michalakes, E. G. Patton, P. J. Riggan, and K. M. Yedinak (2013, August). WRF-Fire: Coupled WeatherWildland Fire Modeling with the Weather Research and Forecasting Model. *Journal of Applied Meteorology and Climatology 52*(1), 16–38.

Fendell, F. E. and M. F. Wolff (2001). *Forest Fires*, Chapter 6, pp. 171–223. Academic Press.

Filippi, J. B., F. Bosseur, C. Mari, C. Lac, P. Le Moigne, B. Cuenot, D. Veynante, D. Cariolle, and J.-H. Balbi (2009). Coupled Atmosphere-Wildland Fire Modelling. *Journal of Advances in Modeling Earth Systems 1*(4).

Linn, R., J. Reisner, J. J. Colman, and J. Winterkamp (2002). Studying wildfire behavior using FIRETEC. *International Journal of Wildland Fire 11*(4), 233–246.

McArthur, A. G. (1966). Weather and grassland fire behaviour. Technical report, Forest Research Instiute, Department of National Development, Commonwealth of Australia.

McArthur, A. G. (1967). Fire behaviour in eucalypt forests. Technical report, Forest Research Institute, Department of National Development, Commonwealth of Australia.

Noble, I. R., G. A. V. Bary, and A. M. Gill (1980). McArthur's fire-danger meters expressed as equations. *Australian Journal of Ecology 5*, 201–203.

Rothermel, R. C. (1972). A mathematical model for predicting fire spread in wildland fuels. Technical report, Forest Service, US Department of Agriculture, Ogden, Utah.

Sethian, J. A. (1985). Curvature and the evolution of fronts. *Communications in Mathematical Physics 101*(4), 487–499.

Sethian, J. A. (1999). *Level Set Methods and Fast Marching Methods: Evolving Interfaces in Computational Geometry, Fluid Mechanics, Compute Vision, and Materials Science* (2 ed.). New York: Cambridge University Press.

Sharples, J. J., R. H. D. McRae, and S. R. Wilkes (2012). Wind-terrain effects on the propagation of wildfires in rugged terrain: fire channelling. *International Journal of Wildland Fire 21*(3), 282–296.

Sharples, J. J., I. N. Towers, G. Wheeler, V.-M. Wheeler, and J.A.McCoy (2013). Modelling fire line merging using plane curvature flow. In *20th International Congress on Modelling and Simulation*, Number 20, pp. 256–262. The Modelling and Simulation Society of Australia and New Zealand Inc.

Simpson, C. C., J. J. Sharples, J. P. Evans, and M. F. McCabe (2013). Large eddy simulation of atypical wildland fire spread on leeward slopes. *International Journal of Wildland Fire 22*(5), 599–614.

Skamarock, W. C., J. B. Klemp, J. Dudhia, D. O. Gill, D. M. Barker, M. Duda, X. Y. Huang, W. Wang, and J. G. Powers (2008). A description of the advanced research WRF version 3. Technical report, National Center for Atmospheric Research, Boulder, Colorado, USA.

Viegas, D. X. (2005). A Mathematical Model For Forest Fires Blowup. *Combustion Science and Technology 177*(1), 27–51.

Viegas, D. X., J. R. Raposo, D. A. Davim, and C. G. Rossa (2012). Study of the jump fire produced by the interaction of two oblique fire fronts. Part 1. Analytical model and validation with no-slope laboratory experiments. *International Journal of Wildland Fire 21*, 843–856.

Weber, R. O. (1989). Analytical Models for Fire Spread Due to Radiation. *Combustion and Flame 78*, 398–408.

Wheeler, V.-M., J. A. McCoy, G. E. Wheeler, and J. J. Sharples (2013). Curvature flows and barriers in fire front modelling. In *20th International Congress on Modelling and Simulation*, Number 20, pp. 297–303. The Modelling and Simulation Society of Australia and New Zealand Inc.